

Journal of Materials Chemistry A

Accepted Manuscript



This is an *Accepted Manuscript*, which has been through the Royal Society of Chemistry peer review process and has been accepted for publication.

Accepted Manuscripts are published online shortly after acceptance, before technical editing, formatting and proof reading. Using this free service, authors can make their results available to the community, in citable form, before we publish the edited article. We will replace this *Accepted Manuscript* with the edited and formatted *Advance Article* as soon as it is available.

You can find more information about *Accepted Manuscripts* in the [Information for Authors](#).

Please note that technical editing may introduce minor changes to the text and/or graphics, which may alter content. The journal's standard [Terms & Conditions](#) and the [Ethical guidelines](#) still apply. In no event shall the Royal Society of Chemistry be held responsible for any errors or omissions in this *Accepted Manuscript* or any consequences arising from the use of any information it contains.

COMMUNICATION

Enhancement of Thermoelectric Properties by Atomic-Scale Percolation in Digenite Cu_xS

Cite this: DOI: 10.1039/x0xx00000x

Qinghui Jiang^{a,*}, Haixue Yan^a, Jibrán Khaliq^a, Yang Shen^b, Kevin Simpson^c, M. J. Reece^{a*}

Received 00th January 2012,
Accepted 00th January 2012

DOI: 10.1039/x0xx00000x

www.rsc.org/

Atomic-scale percolation phenomena of electric and thermal conductivity were found in digenite Cu_xS . Copper ions are randomly located between the closely packed sulphur ions and jump to another position via unoccupied interstices. Near the percolation threshold value ($f_c \sim 0.3$) in the conductive region, a 60% enhancement of zT value can be obtained. This indicates that the percolation phenomena can provide a new strategy to optimize the properties of thermoelectric materials, especially for quasi disordered materials.

Thermoelectric materials^{1, 2} have an important role in solving the global sustainable energy problem to ensure longer energy autonomy, and significantly reduce fuel consumption, and CO_2 emissions.^{3, 4} The challenges focus on developing new materials with higher figure of merit, ZT, values and low cost.⁵ The leading materials are mainly based on bismuth telluride⁶ or lead telluride,⁷ which have high zT value and are suitable for power generation applications or refrigeration. However, tellurium is extremely scarce in the Earth's crust, and tellurium and lead are toxic to human beings. There is an urgent demand to develop nontoxic, inexpensive alternative materials without using rare elements.⁸⁻¹⁰ Cu_xS has been studied for potential application as a p-type semiconductors in solar energy materials with high efficiency.¹¹ Recently, this compound was found to have good thermoelectric properties, which has led to the chalcogenides becoming a new hot spot as low cost and environmentally friendly thermoelectric compounds (for example, Bi_2S_3 ,¹² CuFeS_2 ,¹³ CuSnS ,¹⁴ and BiCuSeO ¹⁵).

In order to improve the efficiency of thermal and electrical conversion, it is necessary to pursue higher zT values. Up to now, three strategies have been successfully adopted to realize higher zT value: (i) band engineering with resonant doping; (ii) the electronic density of states' distortion; and (iii) the reduction of lattice thermal conductivity via increased phonon scattering in nanostructured materials. Percolation theory has been intensively employed to improve the physical properties of heterogeneous materials. According to this theory, there are dramatic changes in the transport properties when minor phase particles form a percolating network in the micro/nanometer scale in composites of two or more phases with

totally different physical properties.¹⁶ Some inorganic/organic thermoelectric nanocomposite materials were fabricated in order to obtain lower thermal conductivity and higher zT value near the critical condition of percolation.^{17, 18} However, the interfaces between the two phases weakened its effect. In this paper, steady atomic-scale percolation was found in digenite Cu_xS compounds with single phase at high temperature (150 °C). The unoccupied copper lattice interstices behave as the minor percolating phase and an obvious enhancement of zT values was obtained near the percolation threshold.

For Cu_xS , there exist various mineral forms in which the locations of Cu atoms in the S lattice are not well identified and their position changes as a function of x . Meanwhile the phase transformations of Cu_xS phases are very sensitive to applied pressure during specimen preparation.¹⁹ Of the copper rich compositions, the experimentally proved stable structures of Cu_xS at room are chalcocite (Cu_2S), djurleite ($\text{Cu}_{1.94}\text{S}$), digenite ($\text{Cu}_{1.8}\text{S}$), and anilite ($\text{Cu}_{1.75}\text{S}$). At higher temperature, the four sulfides are structurally disordered superionic conductors.²⁰ At room temperature, as shown in Figure 1(a), Cu_xS ($1.75 > x > 1$) is a mixture of anilite and covellite phase (CuS); $\text{Cu}_{1.75}\text{S}$ should have the anilite structure, which is naturally a p-type semiconductor due to the Cu vacancies.¹¹ Cu_xS ($1.87 > x > 1.75$) should be the digenite phase. Morimoto et al²¹ observed that the digenite-type solid solution is metastable at room temperature and decomposes into mixtures of anilite and djurleite below 72 °C. Wei S et al used the density-functional theory method to prove that anilite is the most stable structure when $x > 1$. Recently there are a few reports about the synthesis of anilite $\text{Cu}_{1.75}\text{S}$. Simonescu et al prepared anilite $\text{Cu}_{1.75}\text{S}$ nanocrystallites by hydrolytic decomposition of filtrate,²² and there were only three XRD peaks at 26, 32 and 45° which belong to the digenite structure. In our work, all of the Cu_xS (x from 1.7 to 1.9, this ratio is from the starting mixed composition) samples sintered from ball milled powders have similar crystal structure, which can be perfectly indexed as digenite phase (R3m (166) space group, PDF card #47-1748), as shown in Figure 1(b). It indicates that digenite structure can be more stable than anilite when obtained by mechanical alloying. This may be explained by the high impact force¹⁹ generated between the milling balls during the ball milling process making the digenite structure more stable. (However, higher force leads to the appearance of $\text{Cu}_{1.96}\text{S}$, as seen Fig. S1, in

Supplemental Information) Meanwhile, the high cooling rate after the ball milling process may also improve the stability of the digenite structure.

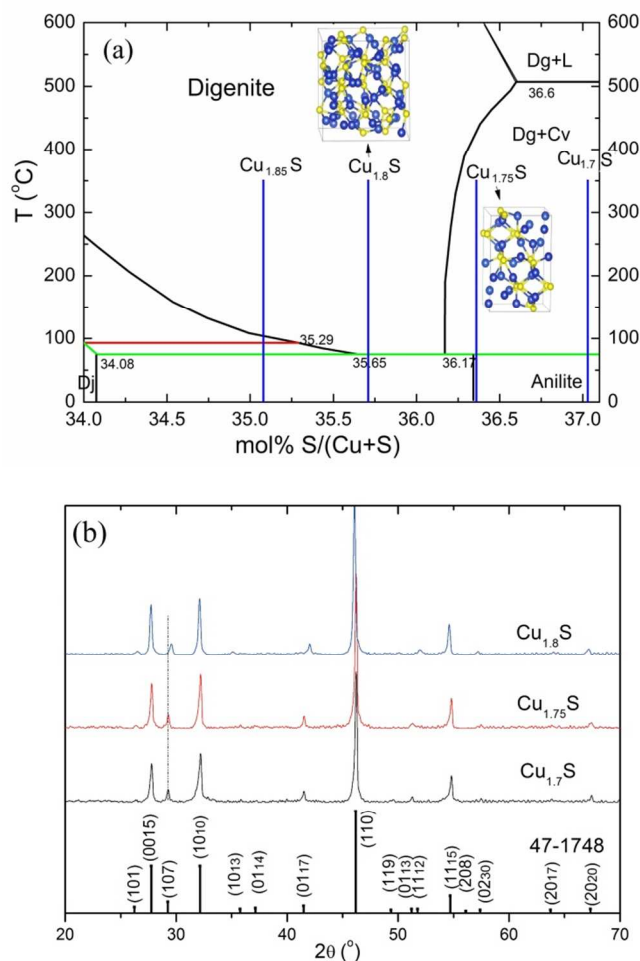


Figure 1. (a) The phase diagram¹⁹ of Cu-S binary system (Ch: chalcocite Cu_2S , Dj: djurleite $\text{Cu}_{1.96}\text{S}$, Dg: Digenite $\text{Cu}_{1.8}\text{S}$,¹¹ An: Anilite $\text{Cu}_{1.75}\text{S}$, Cv: CuS) and (b) XRD patterns of Cu_xS ceramic ($x=1.7$ to 1.8)

For Cu_xS ($1.8 \geq x \geq 1.7$), the low temperature digenite (which is confirmed by Figure 1(b)) can transform to high temperature digenite at ~ 100 °C. For Cu_xS ($x \geq 1.8$), this phase transition is consistent with Figure 1(a).¹⁹ According to the fitting of the XRD data based on the information of PDF 47-1748 (digenite), $\text{Cu}_{1.75}\text{S}$ and $\text{Cu}_{1.7}\text{S}$ have similar lattice parameters ($a=b=3.9238$, $c=48.137$ for $\text{Cu}_{1.75}\text{S}$; $a=b=3.921$, $c=48.132$ for $\text{Cu}_{1.7}\text{S}$), which indicates that the adding of more copper ions into the lattice does not obviously affect the lattice constants. For $\text{Cu}_{1.8}\text{S}$, most peaks also do not move obviously, comparable with $\text{Cu}_{1.75}\text{S}$ and $\text{Cu}_{1.7}\text{S}$. However, some peaks (i.e. $\sim 29^\circ$ for (107)) shift to the right. The lattice constants are $a=b=3.8707$ and $c=48.209$. This illustrates that further adding of the copper ions increases the c axis and simultaneously decreases a and b axes of the unit cell. In the following section, the thermoelectric properties at higher temperature are discussed based on the high temperature digenite phase, in which sulphur ions are hexagonally closed packed (R3m at room temperature) and copper ions are located in the interstices between the sulphur ions.

Liu H L²³ reported the liquid-like behavior of copper ions in Cu_{2-x}Se leads to enhanced zT values. Miller T A *et al.*²⁰ have demonstrated that the same phenomena should lead to similar transport properties for Cu_{2-x}S (above 150–200 °C). Copper ions are randomly distributed in the interstices of the sulphur anions. The compounds exhibit fast-ion conduction with liquid-like mobility,²⁰ and the conduction of copper ions is produced by their jumping to unoccupied interstices. The copper vacancies (i.e. unoccupied interstices) can be regarded as the conductive media in a percolation system. In one sulphur hexagonal unit cell ($6\text{-Cu}_x\text{S}$), there are 6 sulphur atoms and 18 interstices. In a simple rigid model, the content of conductive minor phase (f_v) can be calculated as $(18-6x)/24$. The conductivity of the system near the metal-insulator transition can be described by the percolation equations with power laws ($\sigma \propto (f_c - f_v)^{-5}$ for $f_v < f_c$, and $\sigma \propto (f_v - f_c)^t$ for $f_v > f_c$, where f_v is the volumetric fraction of the conductive second phase, f_c is the percolation threshold, t is the critical exponent in the conducting region, and s is the critical exponent in the insulating region). Due to the limit of the composition ratios studied and the focus on thermoelectric properties, we only consider the t value in the conducting region, as shown in Figure 2.²⁴ For most semiconductors, phonons are the main energy carriers for heat conduction, and there are many models to describe the percolation of thermal conductivity, such as Monte Carlo simulations,²⁵ Fourier's law,²⁶ or a simplified random walk model.²⁷

The fits of the conductivity data give $f_c=0.3$ ($x=1.8$) for electrical conductivity, and $f_c=0.31$ ($x=1.75$) for lattice thermal conductivity, which is higher than the value (0.29) predicted by theory.²⁸ Considering the similar thresholds for electric conductivity (electric scattering) and thermal conductivity (phonon scattering), the maximum zT value should appear near $f_c \sim 0.3$.

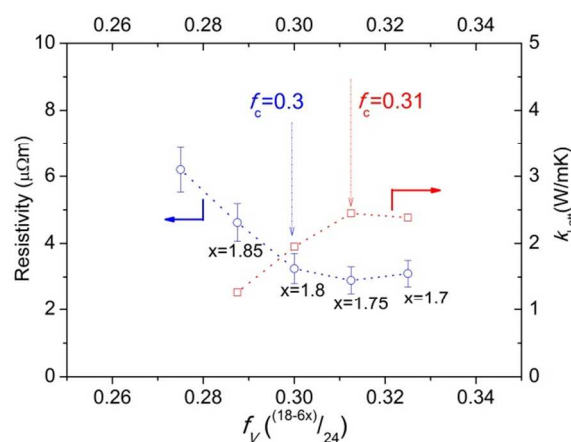


Figure 2. Dependence of the resistivity and lattice thermal conductivity of Cu_xS on the unoccupied interstices fraction $f_v = (18-6x)/24$ at 200 °C

Figure 3 (a) shows the temperature-dependent resistivity data of Cu_xS . The electrical resistivity is determined competitively by carrier concentration and mobility as described by the equation, $1/\rho = pq\mu_p$, where ρ , p , q and μ_p are the electrical resistivity, hole concentration, the electron charge, and the carrier mobility, respectively. In the temperature dependent resistivity curve, there is a minimum at different temperatures, which indicates a phase transition from low temperature digenite to high temperature digenite.²⁹ At higher temperature, the resistivity of compounds increases with increasing temperature due to the boost of the ions'

thermal vibration due to the nature of ionic conductivity. The compounds with high temperature digenite structure exhibit fast-ion conduction and the carrier concentration (Cu^+ and Cu^{2+}) decreases with increasing copper content.

Figure 3(b) shows the temperature dependence of the Seebeck coefficient. The Seebeck coefficient of $\text{Cu}_{1.7}\text{S}$ is about $10 \mu\text{V/K}$ at room temperature, and then decreases with temperature (the value is near zero at 200°C). With increasing temperature, the Seebeck coefficient of $\text{Cu}_{1.75}\text{S}$ increases from 10 to $45 \mu\text{V/K}$ between room temperature and 350°C . This is because of the boost of the ions' thermal vibration decreases the carrier mobility. $\text{Cu}_{1.75}\text{S}$, $\text{Cu}_{1.8}\text{S}$ and $\text{Cu}_{1.85}\text{S}$ have a similar dependence of the Seebeck coefficient with temperature. In these Cu_xS compositions, Cu ions work as charge carriers via Cu vacancies. With x increasing, effective charge carriers density decreases due to low Cu vacancies. Meanwhile, the average distance between Cu vacancies also increased, which resulted in the charge mobility's decrease due to longer distance for Cu ion to jump. As a result, $\text{Cu}_{1.85}\text{S}$ has a higher Seebeck coefficient. For $\text{Cu}_{1.7}\text{S}$, the Seebeck coefficient is much lower, and between 100°C to 250°C this value is near zero. In this temperature range, the

second phase, CuS , may appear and significantly diminish the Seebeck effect according Figure 1(a). As shown in Figure 3(c), at 350°C , $\text{Cu}_{1.75}\text{S}$, $\text{Cu}_{1.8}\text{S}$ and $\text{Cu}_{1.85}\text{S}$ have similar power factors of between 450 and $500 \mu\text{W/mK}^2$. On the contrary, $\text{Cu}_{1.7}\text{S}$ has a much lower power factor, below $100 \mu\text{W/mK}^2$, because it has the lowest Seebeck coefficient in the Cu_xS system.

Figure 4(a) shows the specific heat of $\text{Cu}_{1.8}\text{S}$. There is a maximum peak at $\sim 100^\circ\text{C}$, which indicates the phase transition from low temperature digenite phase to high temperature digenite phase, and this is consistent with the of resistivity data (Figure 3(a)). The reduction of the specific heat with temperature can be explained by local atomic jumping and rearrangement of liquid-like copper ions.²³ The electronic contribution to the thermal conductivity complies with the Wiedeman-Franz (WF) law ($k_{\text{el}}=L\sigma T$, where L is the Lorenz number, taken to be $1.5 \times 10^{-8} \text{W}\Omega\text{K}^{-2}$).⁵ As shown in Figure 4 (b and c), $\text{Cu}_{1.7}\text{S}$ and $\text{Cu}_{1.75}\text{S}$ have similar thermal conductivity (k and k_{lat}). For phonon scattering, the percolation threshold, f_c , is ~ 0.31 . With increasing copper content, more interstitial sites are occupied by Cu ions, and $\text{Cu}_{1.8}\text{S}$ and $\text{Cu}_{1.85}\text{S}$ have a much lower lattice thermal conductivity ($\sim 1\text{-}2 \text{W/mK}$), which indicates that the phonons are scattered by copper ions. As a result, $\text{Cu}_{1.85}\text{S}$ has a lower lattice thermal conductivity, and has the highest zT value of 0.11 at 350°C as shown in Figure 4(d).

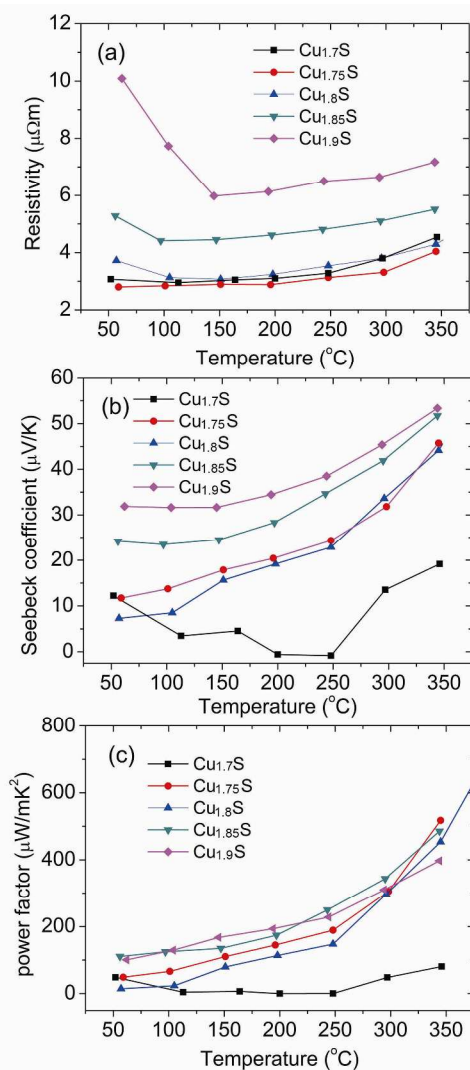


Figure 3. The temperature dependence of: (a) resistivity; (b) Seebeck coefficient; and (c) power factor for Cu_xS .

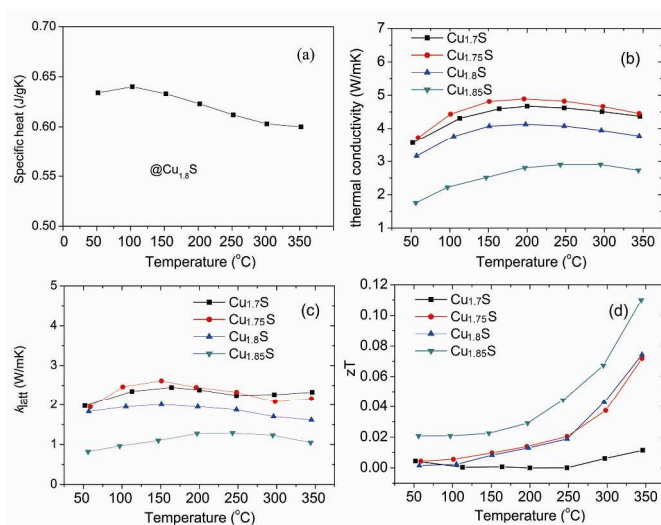


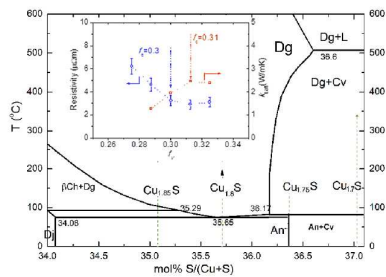
Figure 4. (a) Specific heat of $\text{Cu}_{1.8}\text{S}$. Temperature dependence of thermal conductivity ((b) k ; (c) k_{lat}) and (d) zT value for Cu_xS .

Conclusions

Thermoelectric Cu_xS ($x=1.7, 1.75, 1.8$ and 1.85) with stable Digenite phase were prepared via mechanical alloying and spark plasma sintering. In these non-stoichiometric compounds, the percolation phenomena of the electrical and lattice thermal conductivities with $f_c \sim 0.3$ was found to be due to the disordered distribution of copper vacancies in the interstices of closely packed sulphur ions. Near the threshold of electric conductivity ($f_c \sim 0.3$, i.e. $\text{Cu}_{1.85}\text{S}$), a zT value of ~ 0.11 at 350°C was achieved. The enhancement (60%) produced by percolation can also be used in other disordered materials to optimize their thermoelectric properties.

Notes and references

- ^a School of Engineering and Materials Science, Queen Mary University of London, Mile end road, London, E1 4NS, UK
- ^b State Key Laboratory of New Ceramics and Fine Progressing, Tsinghua University, Beijing 100084, PR China
- ^c European Thermodynamics Ltd, 8 Priory Business Park, Leicester LE8 0RX, UK
- * E-mail: q.jiang@qmul.ac.uk; m.j.reece@qmul.ac.uk
- † Electronic supplementary information (ESI) available: Experimental details, [details of any supplementary information available should be included here]. See DOI: 10.1039/c000000x/
- †† This work was supported by a Marie Curie International Incoming Fellowship of the European Community Human Potential Program under Contract No. PIIF-GA-2010-275223.
- 1 D. M. Rowe, ed. *Thermoelectrics and its Energy Harvesting*, CRC Press, London, 2012.
- 2 K. Koumoto and T. Mori, eds. *Thermoelectric Nanomaterials*, Springer, Berlin Heidelberg, 2013.
- 3 H. Alam and S. Ramakrishna, *Nano Energy*, 2013, **2**, 190-212.
- 4 A. Shakouri, in *Annu. Rev. Mater. Res., Vol 41*, eds. D. R. Clarke and P. Fratzl, 2011, vol. 41, pp. 399-431.
5. T. M. Tritt and M. A. Subramanian, *MRS Bull.*, 2006, **31**, 188-194.
- 6 X. A. Fan, J. Y. Yang, W. Zhu, S. Q. Bao, X. K. Duan, C. J. Xiao and K. Li, *J Phys. D: Appl. Phys.*, 2007, **40**, 5727-5732.
- 7 J. P. Heremans, V. Jovovic, E. S. Toberer, A. Saramat, K. Kurosaki, A. Charoenphakdee, S. Yamanaka and G. J. Snyder, *Science*, 2008, **321**, 554-557.
- 8 C. L. Wan, Y. F. Wang, N. Wang, W. Norimatsu, M. Kusunoki and K. Koumoto, *Sci. Technol. Adv. Mater.*, 2010, **11**, 044306.
- 9 A. Maignan, Y. Breard, E. Guilmeau and F. Gascoin, *J Appl. Phys.*, 2012, **112**, 013716.
- 10 O. Sologub, Y. Matsushita and T. Mori, *Scripta Mater.*, 2013, **68**, 289-292.
- 11 Q. Xu, B. Huang, Y. F. Zhao, Y. F. Yan, R. Noufi and S. H. Wei, *Appl. Phys. Lett.*, 2012, **100**, 061906.
- 12 K. Biswas, L.-D. Zhao and M. G. Kanatzidis, *Adv. Energy Mater.*, 2012, **2**, 634-638.
- 13 N. Tsujii and T. Mori, *Appl. Phys. Expr.*, 2013, **6**, 043001.
- 14 Z. H. Su, K. W. Sun, Z. L. Han, F. Y. Liu, Y. Q. Lai, J. Li and Y. X. Liu, *J Mater. Chem.*, 2012, **22**, 16346-16352.
- 15 Y. Liu, J. Lan, W. Xu, Y. Liu, Y.-L. Pei, B. Cheng, D.-B. Liu, Y.-H. Lin and L.-D. Zhao, *Chem. Commun.*, 2013, **49**, 8075-8077.
- 16 C. W. Nan, Y. Shen and J. Ma, in *Annu. Rev. Mater. Res., Vol 40*, eds. D. R. Clarke, M. Ruhle and F. Zok, 2010, vol. 40, pp. 131-151.
- 17 Y. Du, S. Z. Shen, K. Cai and P. S. Casey, *Prog. Polym. Sci.*, 2012, **37**, 820-841.
- 18 H. Pang, Y.-Y. Piao, Y.-Q. Tan, G.-Y. Jiang, J.-H. Wang and Z.-M. Li, *Mater. Lett.*, 2013, **107**, 150-153.
- 19 D. J. Chakrabarti and D. E. Laughlin, *Bull. Alloy Phase Diagr.*, 1983, **4**, 254-271.
- 20 T. A. Miller, J. S. Wittenberg, H. Wen, S. Connor, Y. Cui and A. M. Lindenberg, *Nat. Commun.*, 2013, **4**, 1369.
- 21 N. Morimoto and K. Koto, *Am. Miner.*, 1970, **55**, 106-117.
- 22 C. M. Simonescu, O. Carp, L. Patron and C. Capatina, *J. Optoelectron. Adv. Mater.*, 2008, **10**, 2700-2702.
- 23 H. L. Liu, X. Shi, F. F. Xu, L. L. Zhang, W. Q. Zhang, L. D. Chen, Q. Li, C. Uher, T. Day and G. J. Snyder, *Nat. Mater.*, 2012, **11**, 422-425.
- 24 Z. M. Dang, Y. H. Lin and C. W. Nan, *Adv. Mater.*, 2003, **15**, 1625-1259.
- 25 W. X. Tian and R. G. Yang, *CMES-Comp. Model. Eng.*, 2008, **24**, 123-141.
- 26 C. W. Nan, G. Liu, Y. H. Lin and M. Li, *Appl. Phys. Lett.*, 2004, **85**, 3549-3551.
- 27 P. Kowalczyk, P. A. Gauden and A. P. Terzyk, *RSC Advances*, 2012, **2**, 4292-4298.
- 28 R. Consiglio, D. R. Baker, G. Paul and H. E. Stanley, *Physica A*, 2003, **319**, 49-55.
- 29 Z. H. Ge, B. P. Zhang, Y. X. Chen, Z. X. Yu, Y. Liu and J. F. Li, *Chem. Commun.*, 2011, **47**, 12697-12699.



Atomic-scale percolation phenomena were found in digenite Cu_xS , providing a new strategy to optimize the properties of thermoelectric materials, especially for quasi disordered materials.